

# Electric and Magnetic fields



Faculty of Physics UW  
Jacek.Szczytko@fuw.edu.pl

# Shubnikov-de Haas effect

## Shubnikov-de Haas effect

Density of states oscillates - falls to 0 for  $\nu = n$  and is highest for  $\nu \approx n + \frac{1}{2}$  - the easiest measurement is the magnetoresistance  $R_{xx}$ .

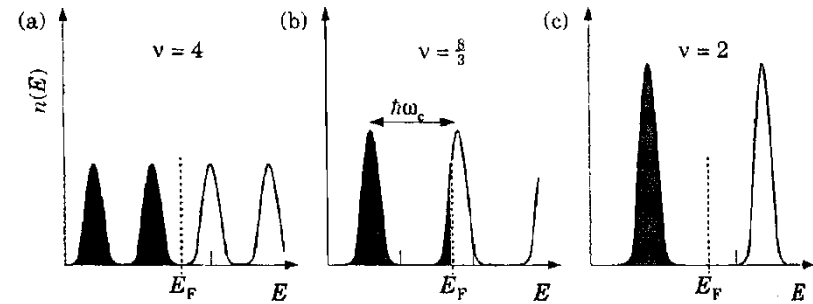


FIGURE 6.8. Occupation of Landau levels in a magnetic field neglecting the spin splitting, showing how the Fermi level moves to maintain a constant density of electrons. The fields are in the ratio

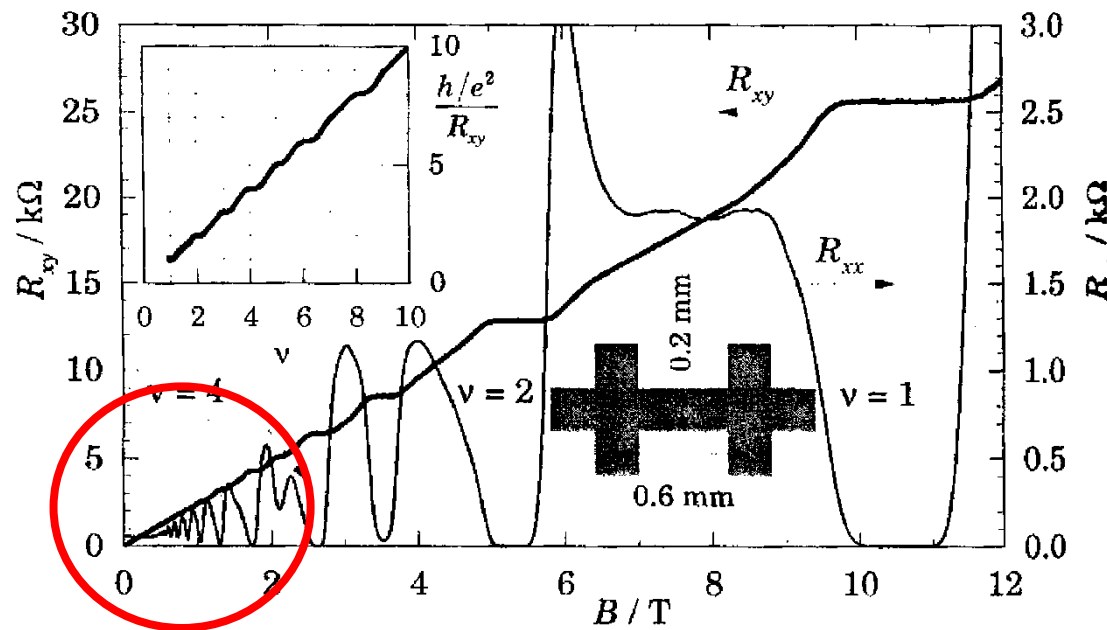
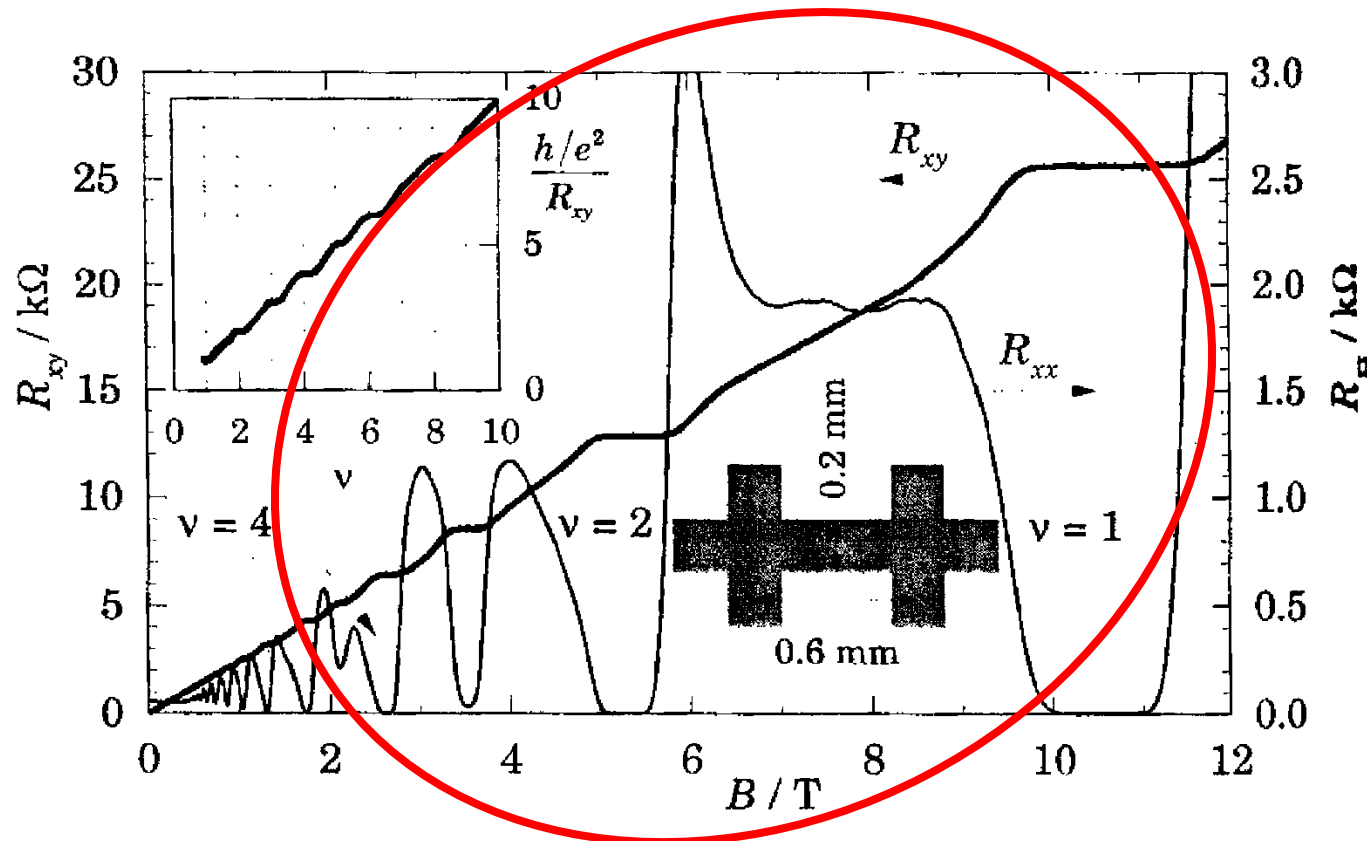


FIGURE 6.10. Longitudinal and transverse (Hall) resistivity,  $R_{xx}$  and  $R_{xy}$ , of a two-dimensional electron gas of density  $n_{2D} = 2.6 \times 10^{15} \text{ nm}^{-2}$  as a function of magnetic field. The measurements were made at  $T = 1.13 \text{ K}$ . The inset shows  $1/R_{xx}$  divided by the quantum unit of conductance  $e^2/h$  as a function of the filling factor  $\nu$ . [Data kindly supplied by Dr A. R. Long, University of Glasgow.]

# Integer Quantum Hall Effect (IQHE)

Integer Quantum Hall effect (IQHE) – for 2D gas: if the Fermi level is located in localized states the Hall resistance (*opór hallowski*) is quantized

$$R_H = \frac{1}{\nu} \frac{h}{e^2}$$



**FIGURE 6.10.** Longitudinal and transverse (Hall) resistivity,  $R_{xx}$  and  $R_{xy}$ , of a two-dimensional electron gas of density  $n_{2D} = 2.6 \times 10^{15} \text{ nm}^{-2}$  as a function of magnetic field. The measurements were made at  $T = 1.13 \text{ K}$ . The inset shows  $1/R_{xx}$  divided by the quantum unit of conductance  $e^2/h$  as a function of the filling factor  $\nu$ . [Data kindly supplied by Dr A. R. Long, University of Glasgow.]

# Integer Quantum Hall Effect (IQHE)

Integer Quantum Hall effect (IQHE) – for 2D gas: if the Fermi level is located in localized states the Hall resistance (*opór hallowski*) is quantized

$$R_H = \frac{1}{\nu} \frac{h}{e^2}$$

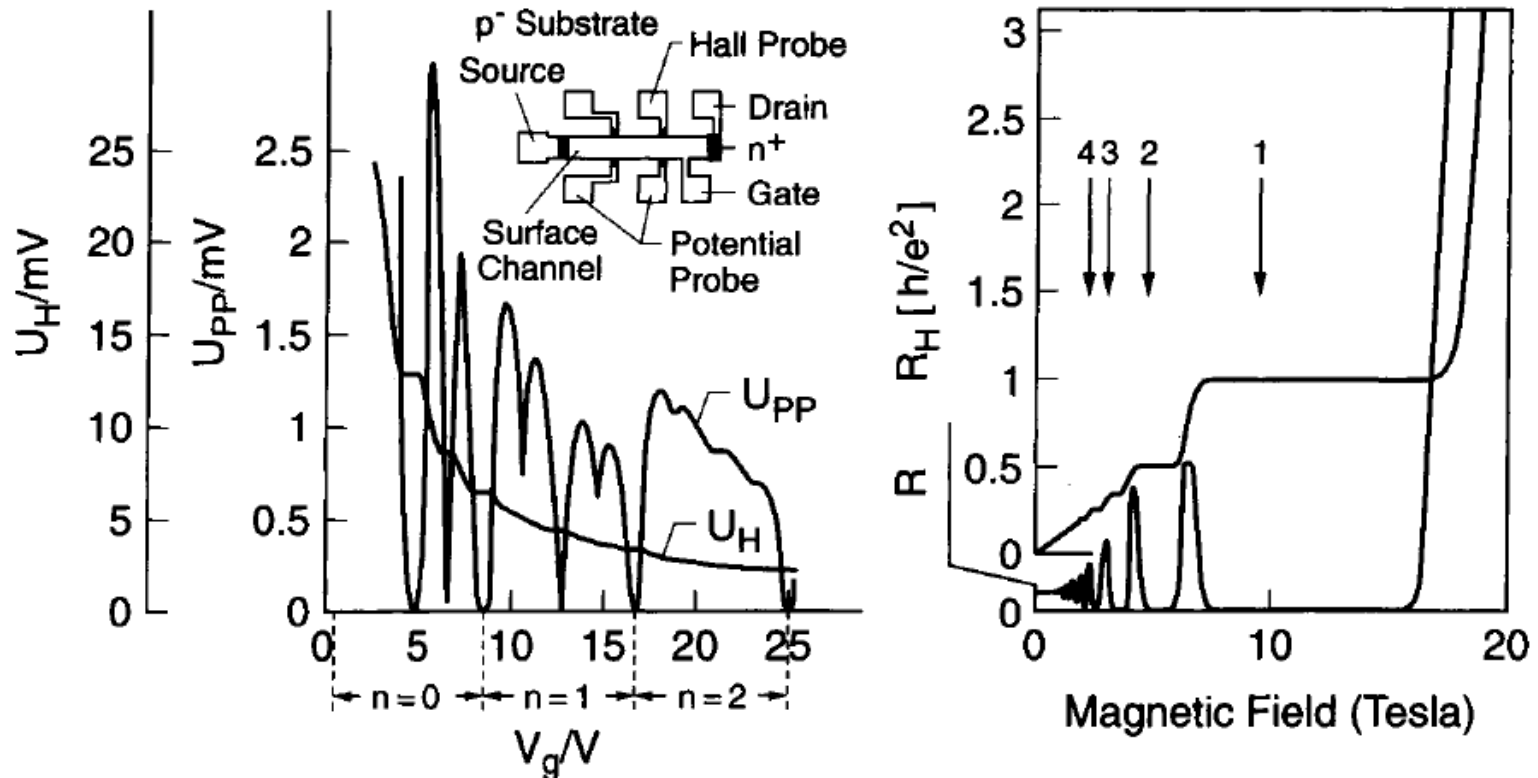


Figure 7. Left panel: original data of the discovery of the integral quantum Hall effect (IQHE) by Klaus von Klitzing in 1980 in the two-dimensional electron system of a silicon MOSFET transistor. Instead of a smooth curve he observed plateaus in the Hall voltage ( $U_H$ ) and found concomitant deep minima in the magneto resistance ( $U_{PP}$ ). The horizontal axis represents gate voltage ( $V_G$ ) which varies the carrier density,  $n$ . The right panel shows equivalent data taken on a two-dimensional electron system in GaAs/AlGaAs. Since these data are plotted versus magnetic field they can directly be compared to Edwin Hall's data of Fig. 6. Rather than the linear dependence of the Hall resistance on magnetic field of Fig. 6, these data show wide plateaus in  $R_H$  and in addition deep minima in  $R$ .

Stromer, Nobel Lecture

# Quantum Hall Effect



The Nobel Prize in Physics 1985  
Klaus von Klitzing

The Nobel Prize in Physics 1985

Nobel Prize Award Ceremony

Klaus von Klitzing



Klaus von Klitzing

The Nobel Prize in Physics 1985 was awarded to Klaus von Klitzing *"for the discovery of the quantized Hall effect"*.

# Quantum Hall Effect



## The Nobel Prize in Physics 1998

Robert B. Laughlin, Horst L. Störmer, Daniel C. Tsui

The Nobel Prize in Physics 1998

Nobel Prize Award Ceremony

Robert B. Laughlin

Horst L. Störmer

Daniel C. Tsui



Robert B. Laughlin



Horst L. Störmer



Daniel C. Tsui

The Nobel Prize in Physics 1998 was awarded jointly to Robert B. Laughlin, Horst L. Störmer and Daniel C. Tsui *"for their discovery of a new form of quantum fluid with fractionally charged excitations"*.

# Quantum Hall Effect

## Integer Quantum Hall effect (IQHE)

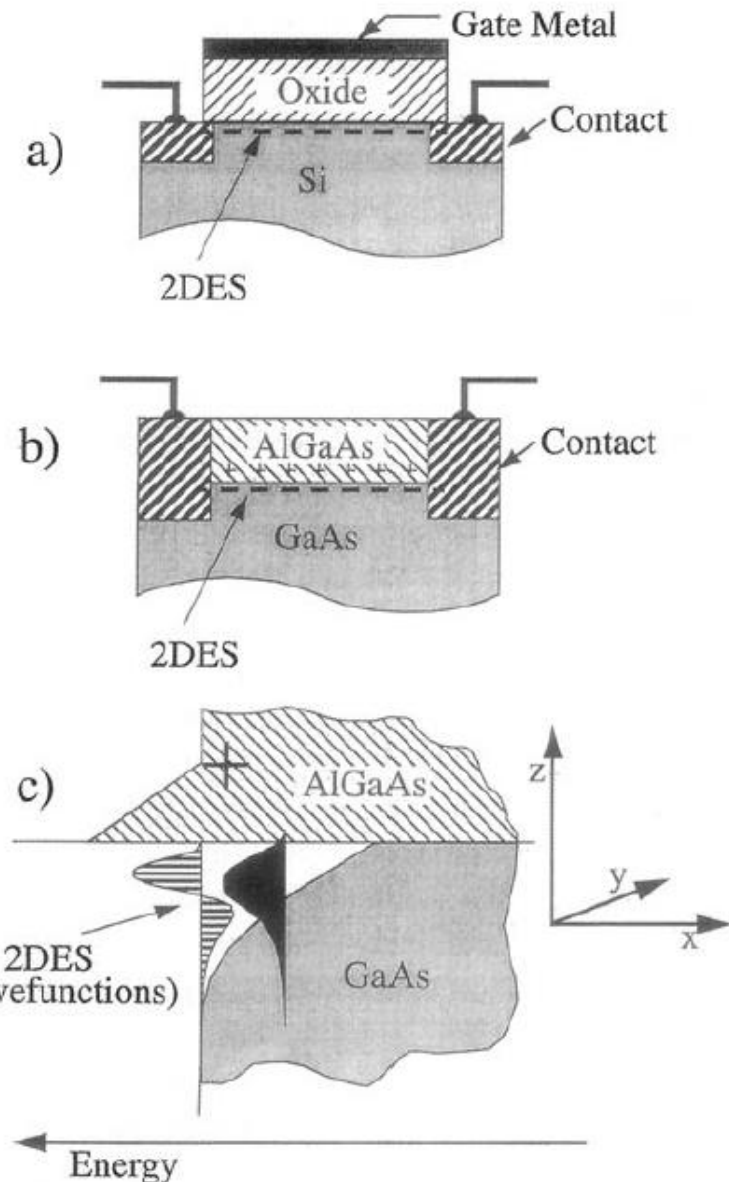
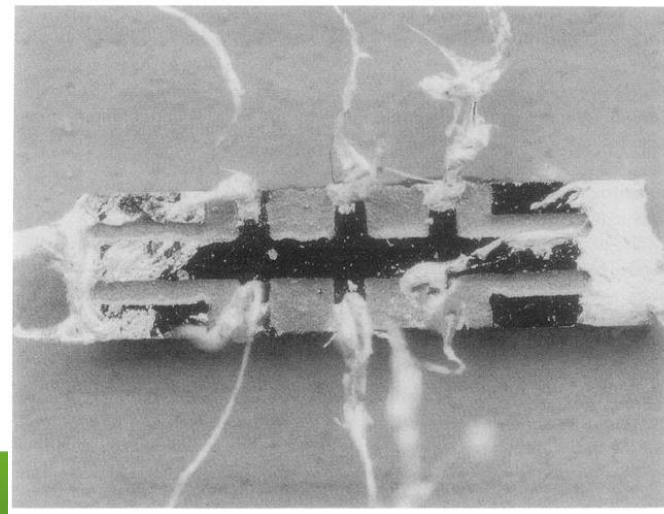
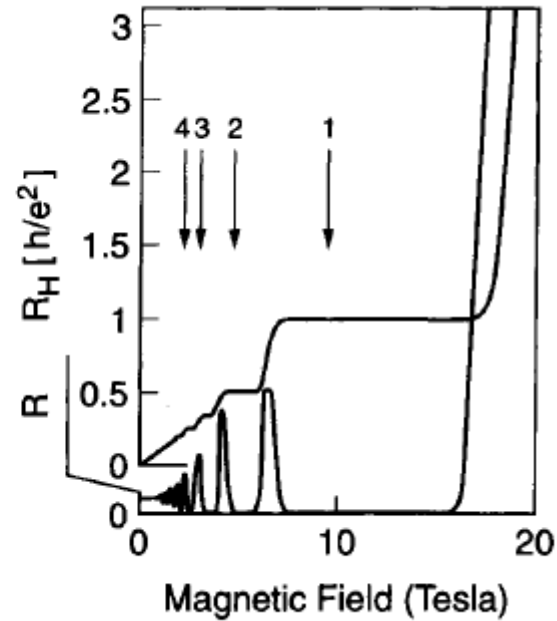
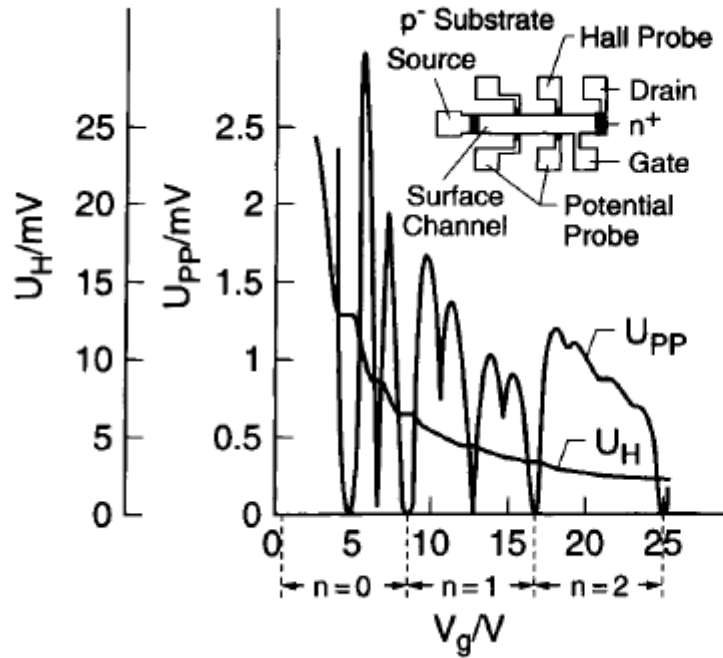


Figure 1 a). Schematic drawings of a silicon Metal Oxide Semiconductor Field Effect Transistor (MOSFET). The two-dimensional electron system (2DES) resides at the interface between silicon and silicon oxide. Electrons are held against the oxide by the electric field from the gate metal. b) Schematic drawings of a modulation-doped gallium arsenide/aluminum gallium arsenide (GaAs/AlGaAs) heterojunction. The 2DES resides at the interface between GaAs and AlGaAs. Electrons are held against the AlGaAs by the electric field from the charged silicon dopants (+) in the AlGaAs. c). Energetic condition in the modulation-doped structure (very similar to the condition in the MOSFET). Energy increases to the left. Electrons are trapped in the triangular-shaped quantum-well at the interface. They assume discrete energy states in the  $z$ -direction (black and horizontally striped). At low temperatures and low electron concentration only the lowest (black) electron state is occupied. The electrons are totally confined in the  $z$ -direction but can move freely in the  $x$ - $y$ -plane.

Horst Stormer, *Nobel Lecture*

# Quantum Hall Effect



Horst Stormer, *Nobel Lecture*

# Quantum Hall Effect

VOLUME 45, NUMBER 6

PHYSICAL REVIEW LETTERS

11 AUGUST 1980

## New Method for High-Accuracy Determination of the Fine-Structure Constant Based on Quantized Hall Resistance

K. v. Klitzing

Physikalisches Institut der Universität Würzburg, D-8700 Würzburg, Federal Republic of Germany, and  
Hochfeld-Magnettlabor des Max-Planck-Instituts für Festkörperforschung, F-38042 Grenoble, France

and

G. Dorda

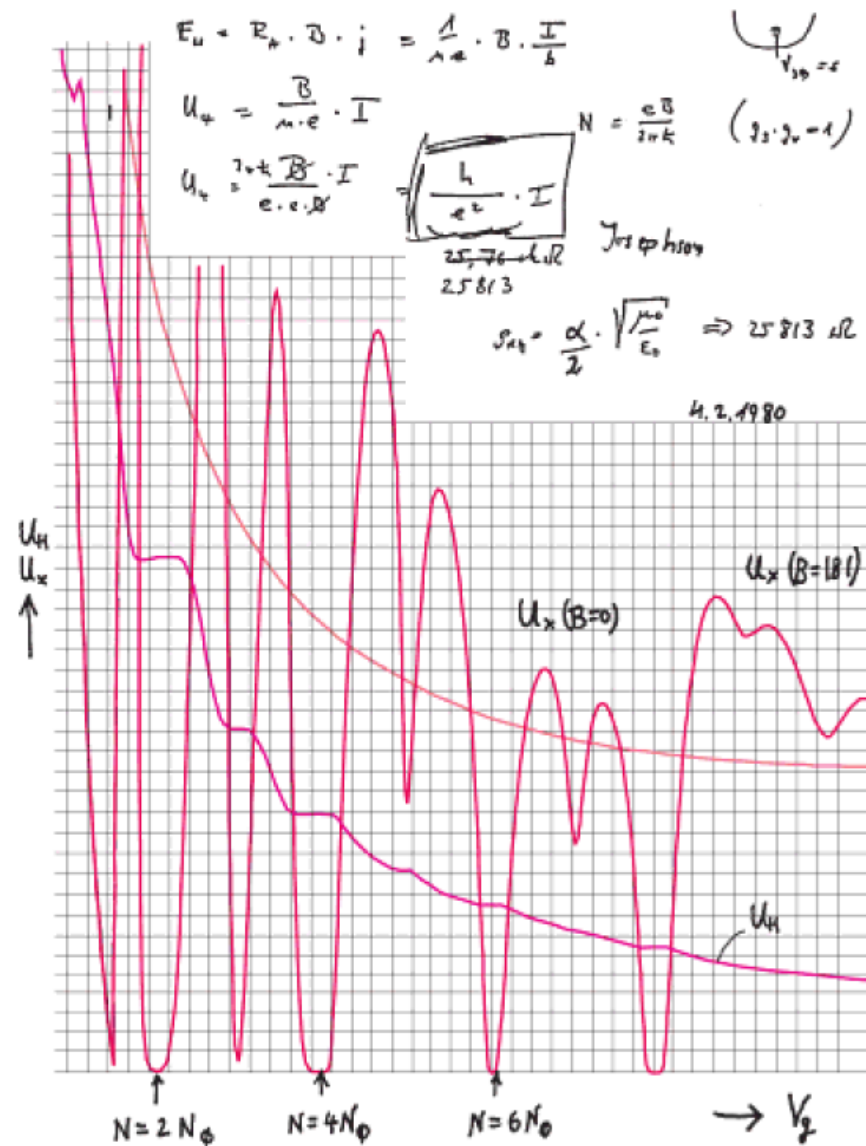
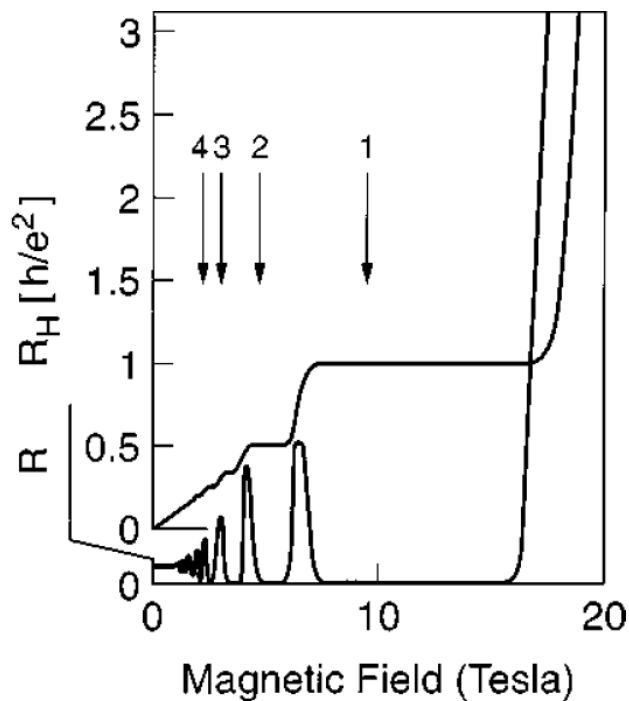
Forschungslaboratorien der Siemens AG, D-8000 München, Federal Republic of Germany

and

M. Pepper

Cavendish Laboratory, Cambridge CB3 0HE, United Kingdom

(Received 30 May 1980)



# Quantum Hall Effect

VOLUME 45, NUMBER 6

PHYSICAL REVIEW LETTERS

11 AUGUST 1980

## New Method for High-Accuracy Determination of the Fine-Structure Constant Based on Quantized Hall Resistance

K. v. Klitzing

*Physikalisches Institut der Universität Würzburg, D-8700 Würzburg, Federal Republic of Germany, and  
Hochfeld-Magnetlabor des Max-Planck-Instituts für Festkörperforschung, F-38042 Grenoble, France*

and

G. Dorda

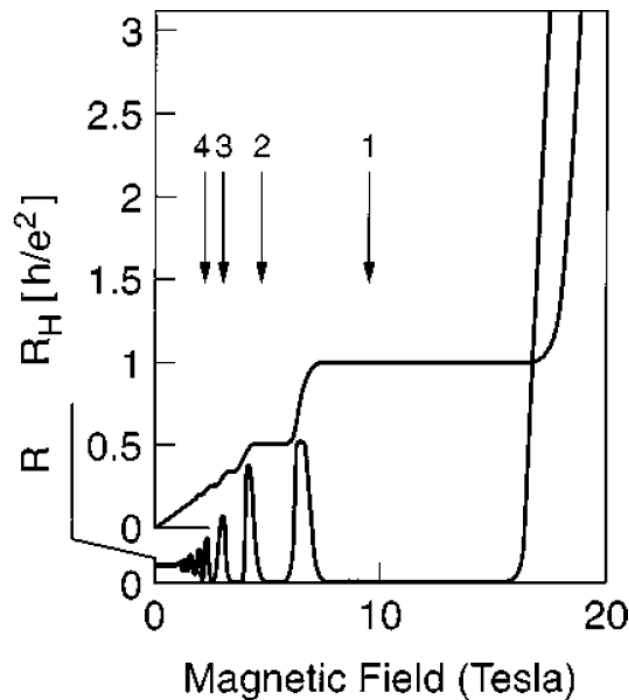
*Forschungslaboratorien der Siemens AG, D-8000 München, Federal Republic of Germany*

and

M. Pepper

*Cavendish Laboratory, Cambridge CB3 0HE, United Kingdom*

(Received 30 May 1980)



## Conductivity tensor

$$\sigma = \begin{pmatrix} \sigma_L & -\sigma_T \\ \sigma_T & \sigma_L \end{pmatrix} = \frac{\sigma_0}{1 + \omega_c^2 \tau^2} \begin{pmatrix} 1 & \omega_c \tau \\ -\omega_c \tau & 1 \end{pmatrix}$$

## Full resistivity tensor

$$\rho = \sigma^{-1} = \frac{1}{ne\mu} \begin{pmatrix} 1 & -s & 0 \\ s & 1 & 0 \\ 0 & 0 & 1 \end{pmatrix}$$

$$\rho = \frac{1}{\sigma_L^2 + \sigma_T^2} \begin{pmatrix} \sigma_L & -\sigma_T \\ \sigma_T & \sigma_L \end{pmatrix} = \frac{1}{\sigma_0} \begin{pmatrix} 1 & -\omega_c \tau \\ \omega_c \tau & 1 \end{pmatrix}$$

For large magnetic fields  $|\sigma_T| \gg \sigma_L$

$$\rho = \frac{1}{\sigma_L^2 + \sigma_T^2} \begin{pmatrix} \sigma_L & -\sigma_T \\ \sigma_T & \sigma_L \end{pmatrix} \approx \begin{pmatrix} \sigma_L/\sigma_T^2 & -1/\sigma_T \\ 1/\sigma_T & \sigma_L/\sigma_T^2 \end{pmatrix}$$

thus  $\rho \sim \sigma_L$  !

# Hall Effect

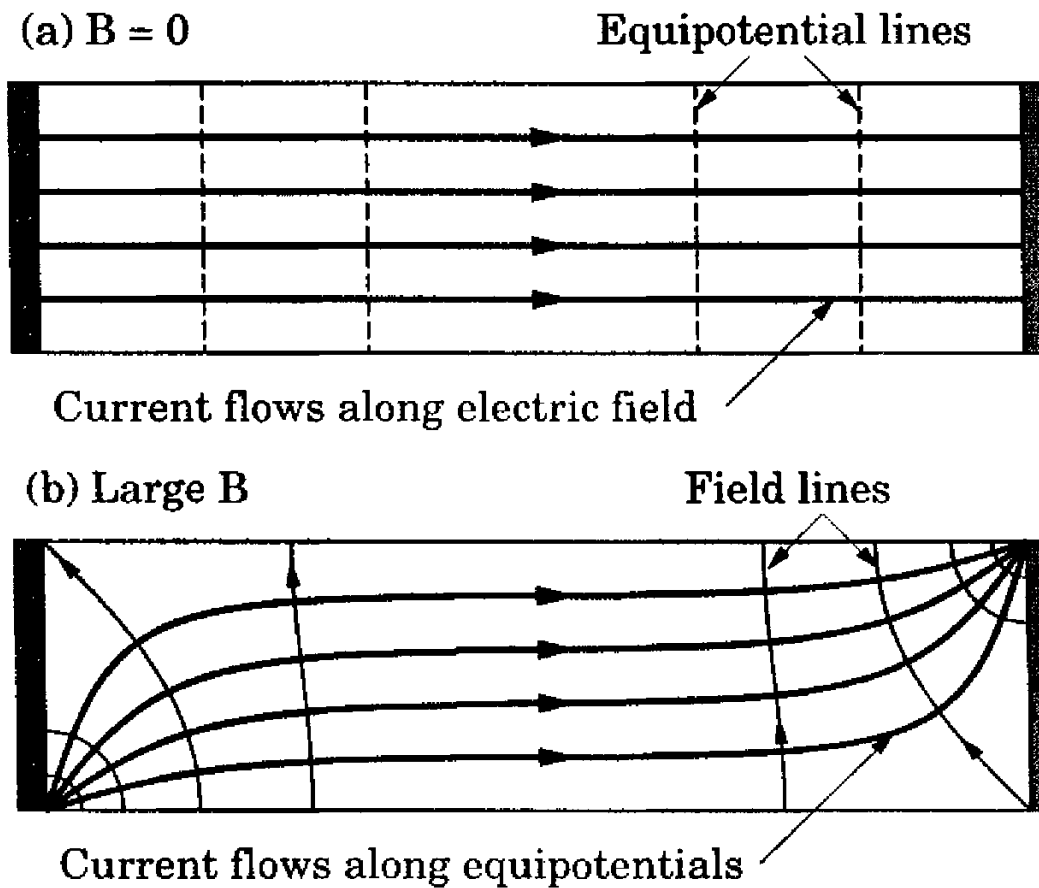


**FIGURE 6.6.** Electric field, current flow, and equipotentials inside a long rectangular sample with contacts across each end. (a) In the absence of an electric field the current is uniform throughout the sample and runs along the electric field. (b) In a strong magnetic field, where  $|\sigma_T| \gg \sigma_L$ , the current runs along equipotentials.

# Quantized conductance

$$G = \frac{dI}{dU} = \frac{2e^2}{h} \int_{E_L}^{\infty} \frac{\partial f(E, \mu)}{\partial E} T(E) dE \approx \frac{2e^2}{h} T(\mu) = G_0 T(\mu)$$

$$\frac{e^2}{h} = 38,7 \mu S$$

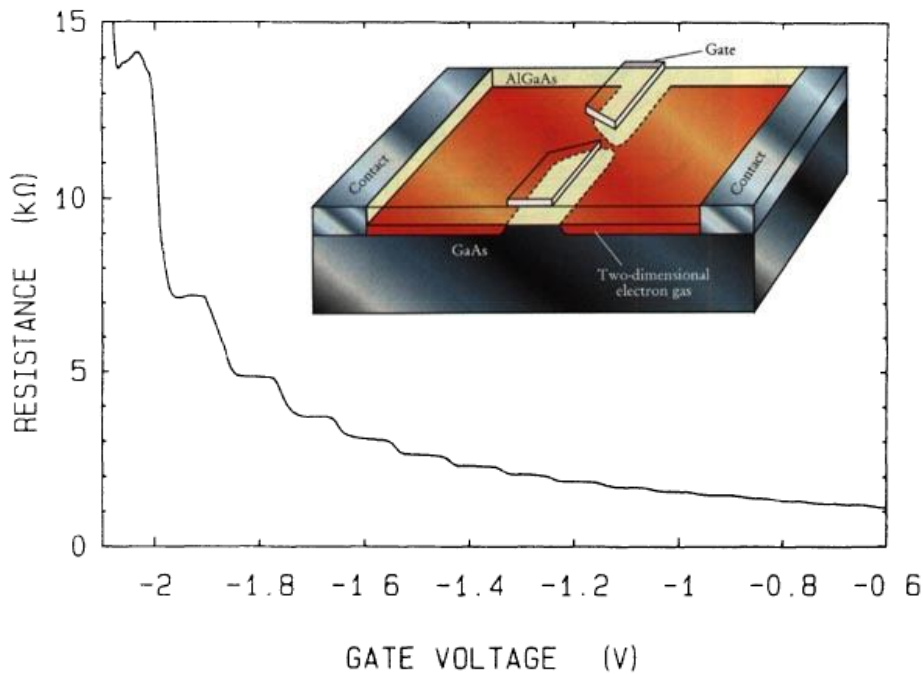


FIG. 1. Point-contact resistance as a function of gate voltage at 0.6 K. Inset: Point-contact layout.

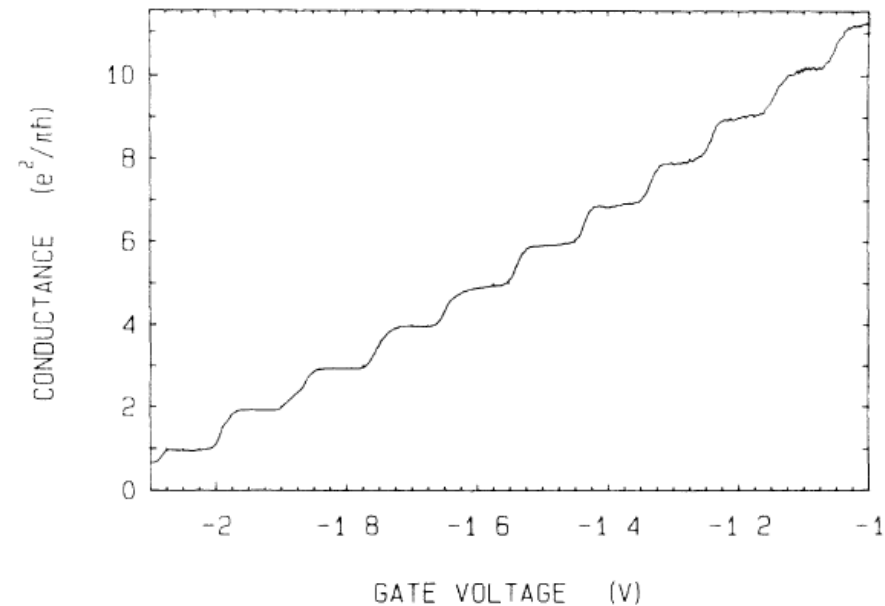


FIG. 2. Point-contact conductance as a function of gate voltage, obtained from the data of Fig. 1. The conductance is a function of the lead resistance. The conductance is quantized at multiples of  $e^2/\pi h$ .

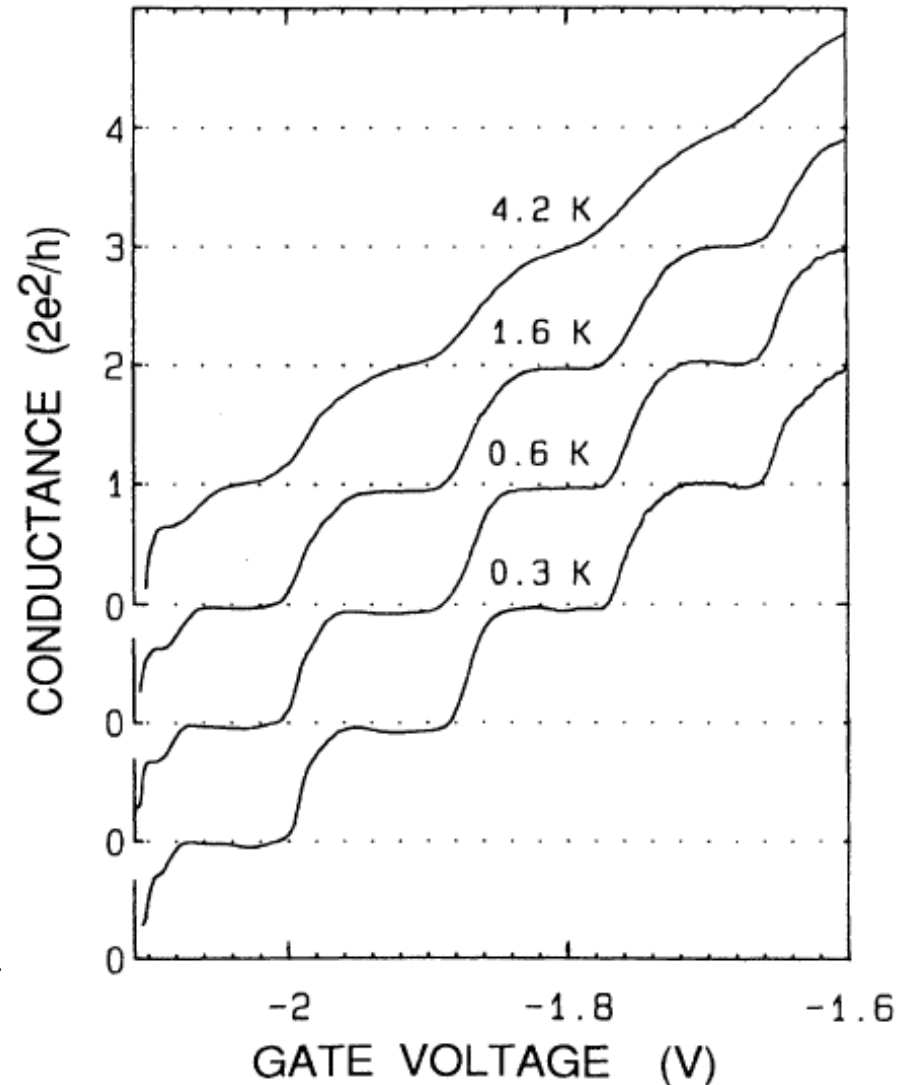
**Reminder**

B. J. van Wees et al. *Quantized conductance of point contacts in a two-dimensional electron gas*. Phys. Rev. Lett. **60**, 848–850 (1988)

# Quantized conductance

$$G = \frac{2e^2}{h} T(\mu) = G_0 T(\mu)$$

Reminder



B. J. van Wees et al. *Quantum ballistic and adiabatic electron transport studied with quantum point contacts* Phys. Rev. B 43, 12431–12453 (1991)

FIG. 6. Breakdown of the conductance quantization due to temperature averaging. The curves have been offset for clarity.

# Electric and magnetic fields

Motion of the electron in crossed fields: electric  $\vec{E} = (E, 0, 0)$  and magnetic  $\vec{B} = (0, 0, B)$  is encircled by cycloid :

$$x(t) = -\frac{mE}{eB^2} (1 - \cos \omega_c t)$$

$$y(t) = -\frac{mE}{eB^2} (\omega_c t - \sin \omega_c t)$$

Details of the movement depends on the initial conditions

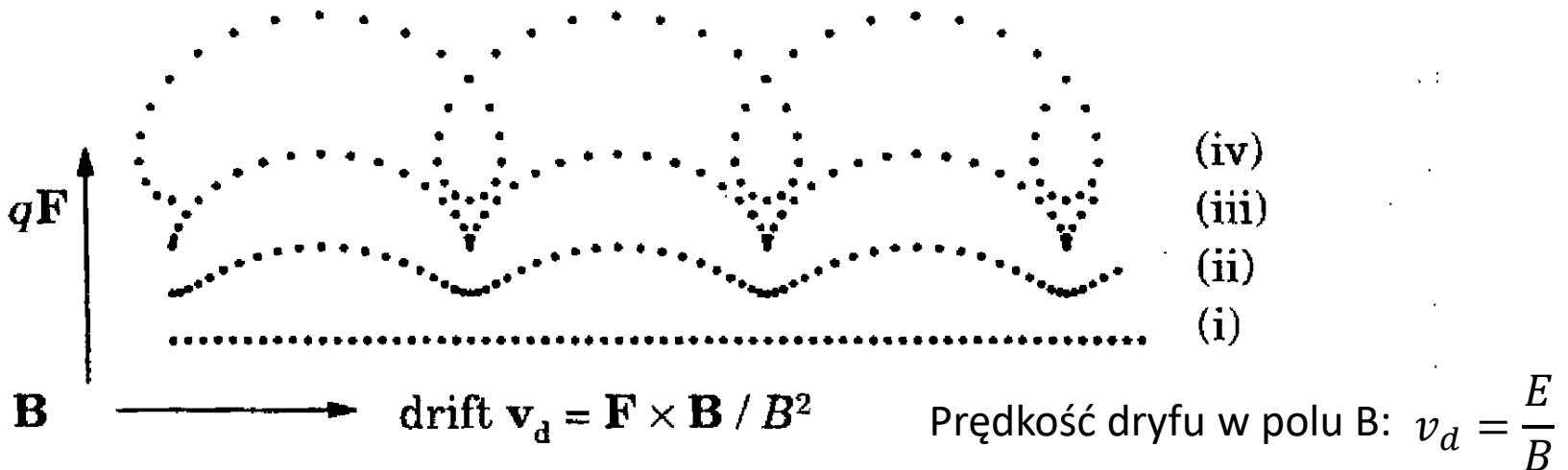


**FIGURE 6.11.** Classical motion of a charged particle in crossed electric and magnetic fields, with  $\mathbf{B}$  normal to the page and equal intervals of time between the symbols. The curves correspond to different initial velocities and energies, with (iii) showing the cycloid for a particle initially at rest.

# Homogenous magnetic field

$$\left[ -\frac{\hbar^2}{2m} \nabla^2 - \frac{ie\hbar}{m} Bx \frac{\partial}{\partial y} + \frac{(eBx)^2}{2m} + U(z) \right] \psi(\vec{r}) = E\psi(\vec{r})$$

Vector potential does not depend on  $y$ , we can assume the function of the form:

$$\psi(\vec{r}) = w(z)u(x) \exp(ik_y y)$$

$$\left[ -\frac{\hbar^2}{2m} \frac{d^2}{dx^2} + \frac{1}{2} m \omega_c^2 \left( x + \frac{\hbar k_y}{eB} \right)^2 \right] u(x) = \varepsilon u(x)$$

$$\omega_c = \left| \frac{eB}{m} \right|$$

$$R_c = \frac{v}{\omega_c} = \frac{\sqrt{2mE}}{|eB|}$$

Cyclotron frequency

Cyclotron radius (*gyroradius*)

$k_y$  wave vector. What interesting in  $\varepsilon$  THERE IS NO  $k_y$ .

The parabolic potential of the form of  $x_k = -\hbar k_y / eB$

**Reminder**

# Electric and magnetic fields

$$\left[ -\frac{\hbar^2}{2m} \nabla^2 - \frac{ie\hbar}{m} Bx \frac{\partial}{\partial y} + \frac{(eBx)^2}{2m} + eEx \right] \psi(\vec{r}) = E\psi(\vec{r})$$

Vector potential does not depend on  $y$ , we can assume:  $\psi(\vec{r}) = w(z)u(x) \exp(ik_y y)$

$$\left[ -\frac{\hbar^2}{2m} \frac{d^2}{dx^2} + \frac{1}{2} m \omega_c^2 \left( x + \frac{\hbar k_y}{eB} + \frac{Ee}{m\omega_c^2} \right)^2 - \frac{\hbar k E}{B} - \frac{mE^2}{2B^2} \right] u(x) = \varepsilon u(x)$$

Factors „added” in order to get  $eE$  after expanding  $(\dots)^2$

Parabolic potential shifted by

$$x_k = - \left( \frac{\hbar k_y}{eB} + \frac{Ee}{m\omega_c^2} \right) = \frac{mv_d - \hbar k}{eB}$$

$$v_d = \frac{E_x}{B_z}$$

$$\begin{aligned} \varepsilon_{nk} &= \left( n - \frac{1}{2} \right) \hbar \omega_c - \frac{\hbar k E}{B} - \frac{mE^2}{2B^2} = \\ &= \left( n - \frac{1}{2} \right) \hbar \omega_c - eE x_k - \frac{1}{2} m v_D^2 \end{aligned}$$

$$J_y = -en_{2D} v_D = en_{2D} \frac{E_x}{B_z} \Rightarrow \sigma_{xx} = \sigma_L = 0$$

$$\rho_T = 1/\sigma_T = B_z/en_{2D} \quad (\text{classical Hall effect})$$

# Electric and magnetic fields

Parabolic potential depends on magnetic field and  $k_y$

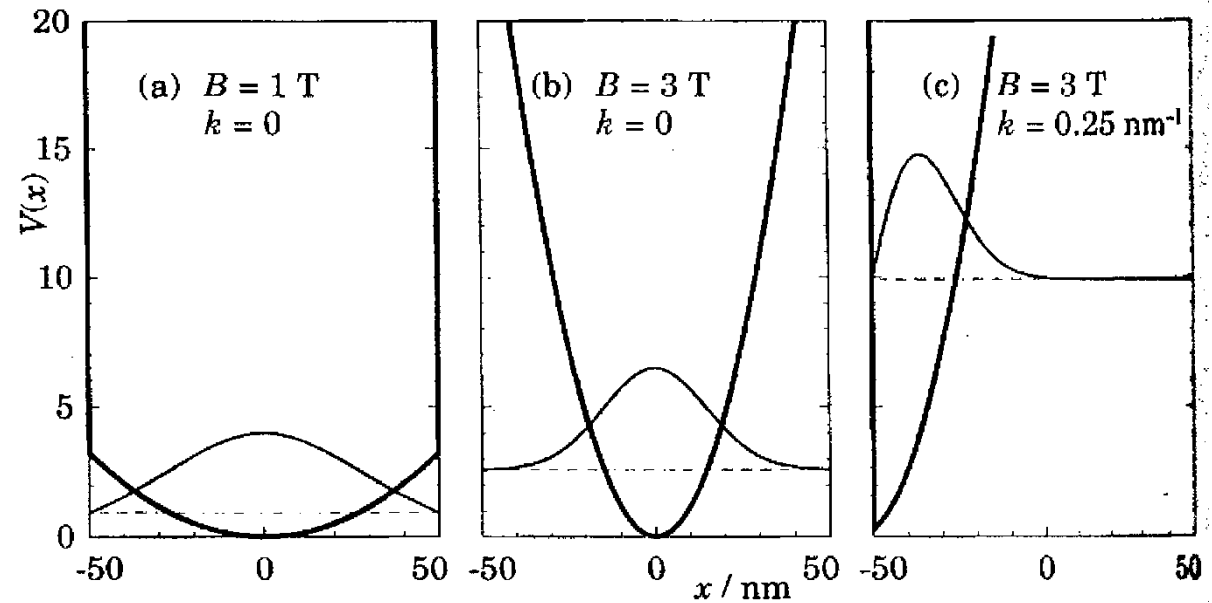
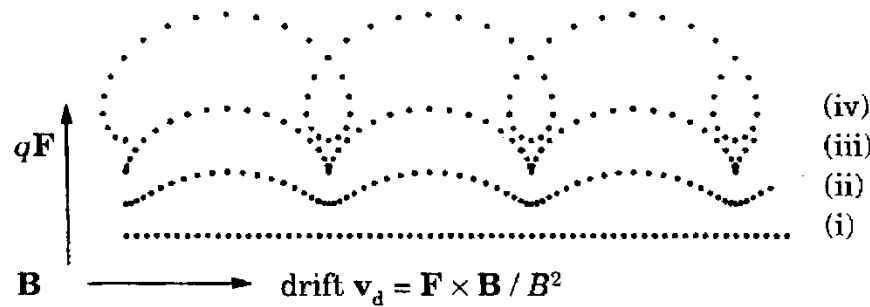


FIGURE 6.13. Potential energy and lowest eigenstate in a magnetic field for an electron with wave number  $k$  in a hard-walled wire of width  $0.1 \mu\text{m}$  in GaAs.



$$v_d = \frac{E}{B}$$

FIGURE 6.11. Classical motion of a charged particle in crossed electric and magnetic fields, with  $\mathbf{B}$  normal to the page and equal intervals of time between the symbols. The curves correspond to different initial velocities and energies, with (iii) showing the cycloid for a particle initially at rest.

# Electric and magnetic fields

Parabolic potential depends on magnetic field and  $k_y$

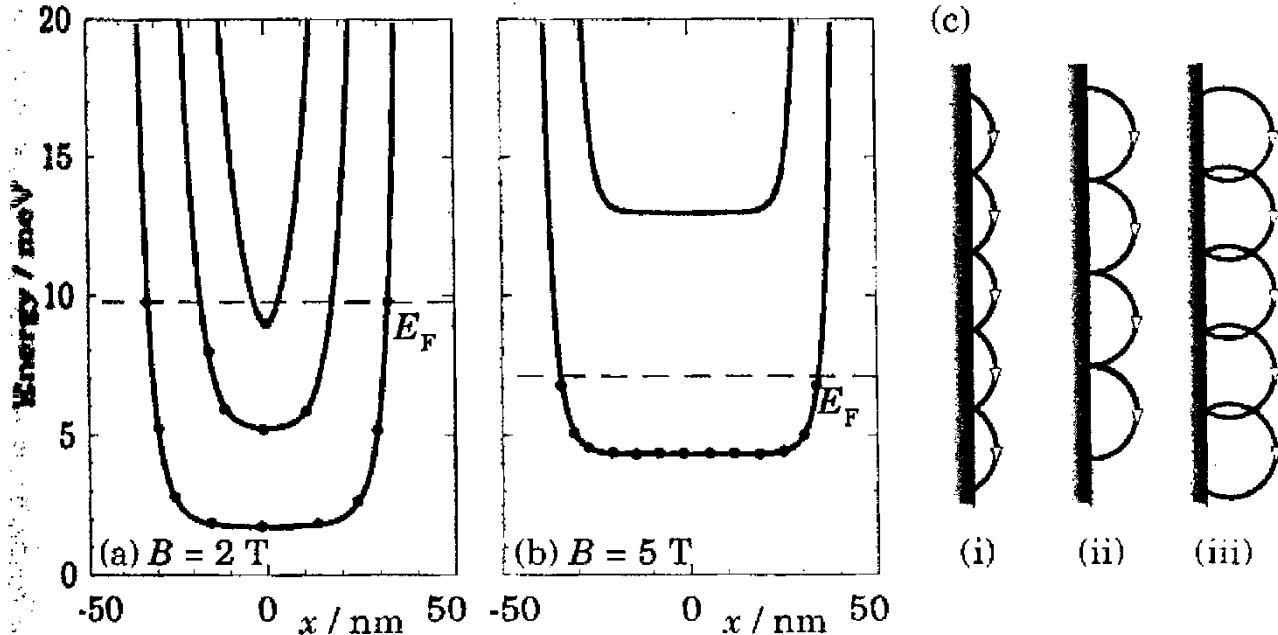
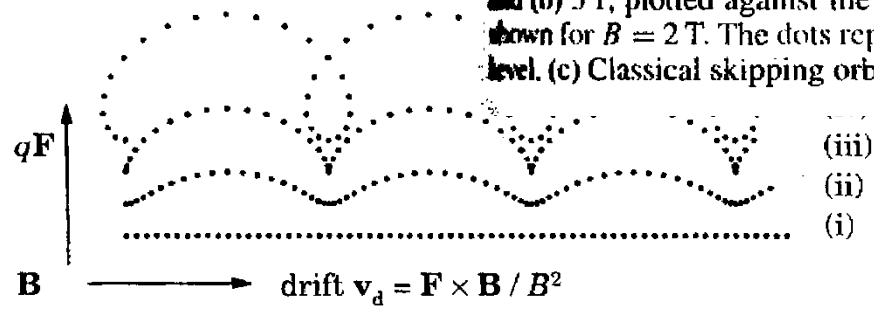


FIGURE 6.14. Energies  $\epsilon_{nk}(B)$  of electrons in a hard-walled wire in a magnetic field of (a) 2 T and (b) 5 T, plotted against the guiding centre  $\langle x_{nk} \rangle$ . For clarity, only the lowest three bands are shown for  $B = 2$  T. The dots represent some of the occupied states and the dashed line is the Fermi level. (c) Classical skipping orbits along the edge of a wire.



$$v_d = \frac{E}{B}$$

FIGURE 6.11. Classical motion of a charged particle in crossed electric and magnetic fields, with  $\mathbf{B}$  normal to the page and equal intervals of time between the symbols. The curves correspond to different initial velocities and energies, with (iii) showing the cycloid for a particle initially at rest.

# Electric and magnetic fields

Parabolic potential depends on magnetic field and  $k_y$

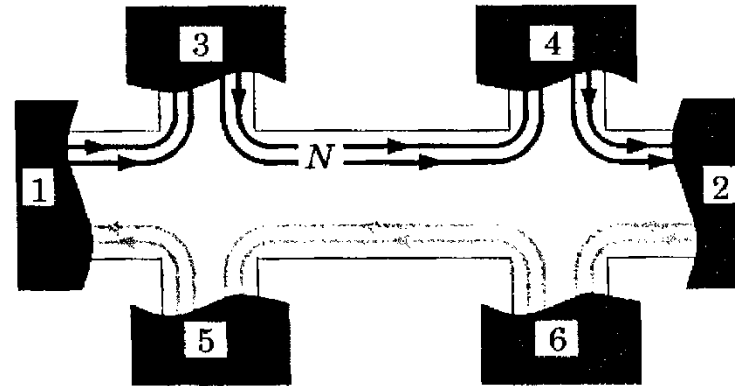


**FIGURE 6.18.** A Hall bar in a strong magnetic field, showing the propagation of edge states. A negative bias on contact 1 injects extra electrons into the  $N$  edge states that leave it (only two of which are drawn); the electrons depart through the other current probe (2).

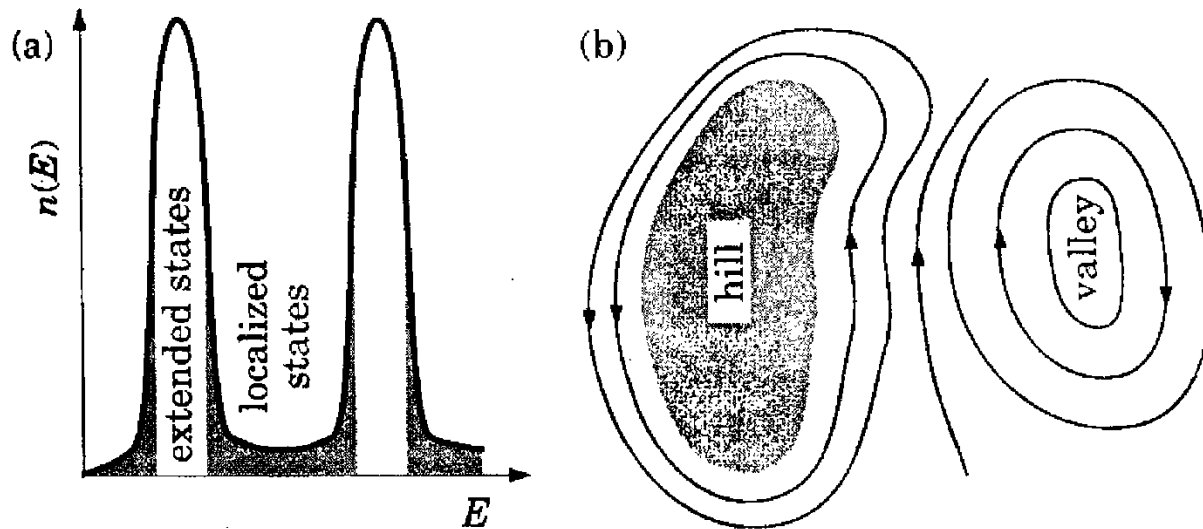


**FIGURE 6.19.** (a) Density of states of a Landau level in a disordered system showing a band of extended states in the centre of each level with localized states in between. (b) Edge states localized in a slowly varying potential, with a hill on the left and a hollow on the right.

# Electric and magnetic fields

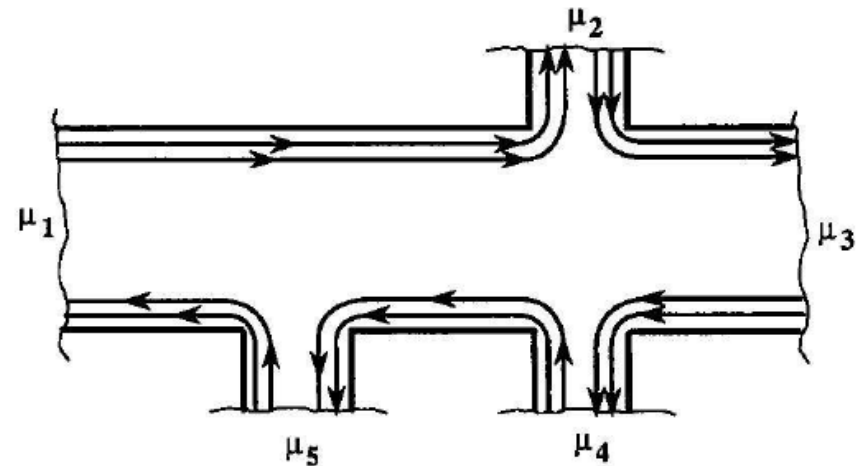
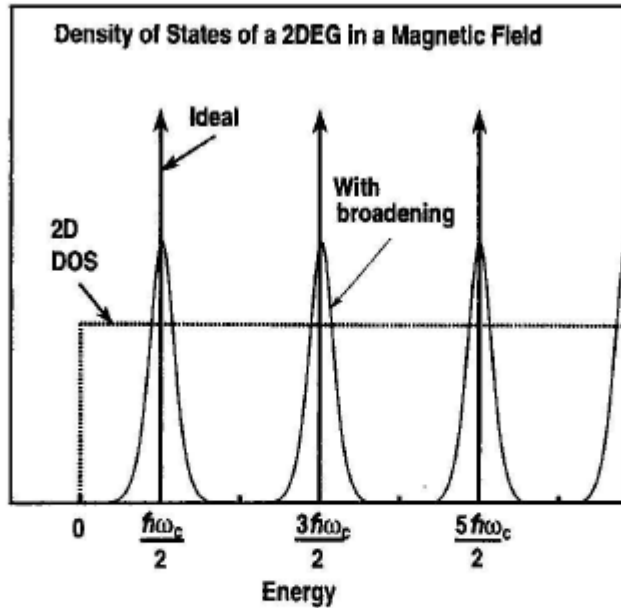


Figure 5.5: Hall bar with five terminals each with chemical potential  $\mu_i$ . The Fermi energy is set in the Quantum Hall regime such that there are two edge-channels connecting the terminals. Picture from Ferry & Goodnick.

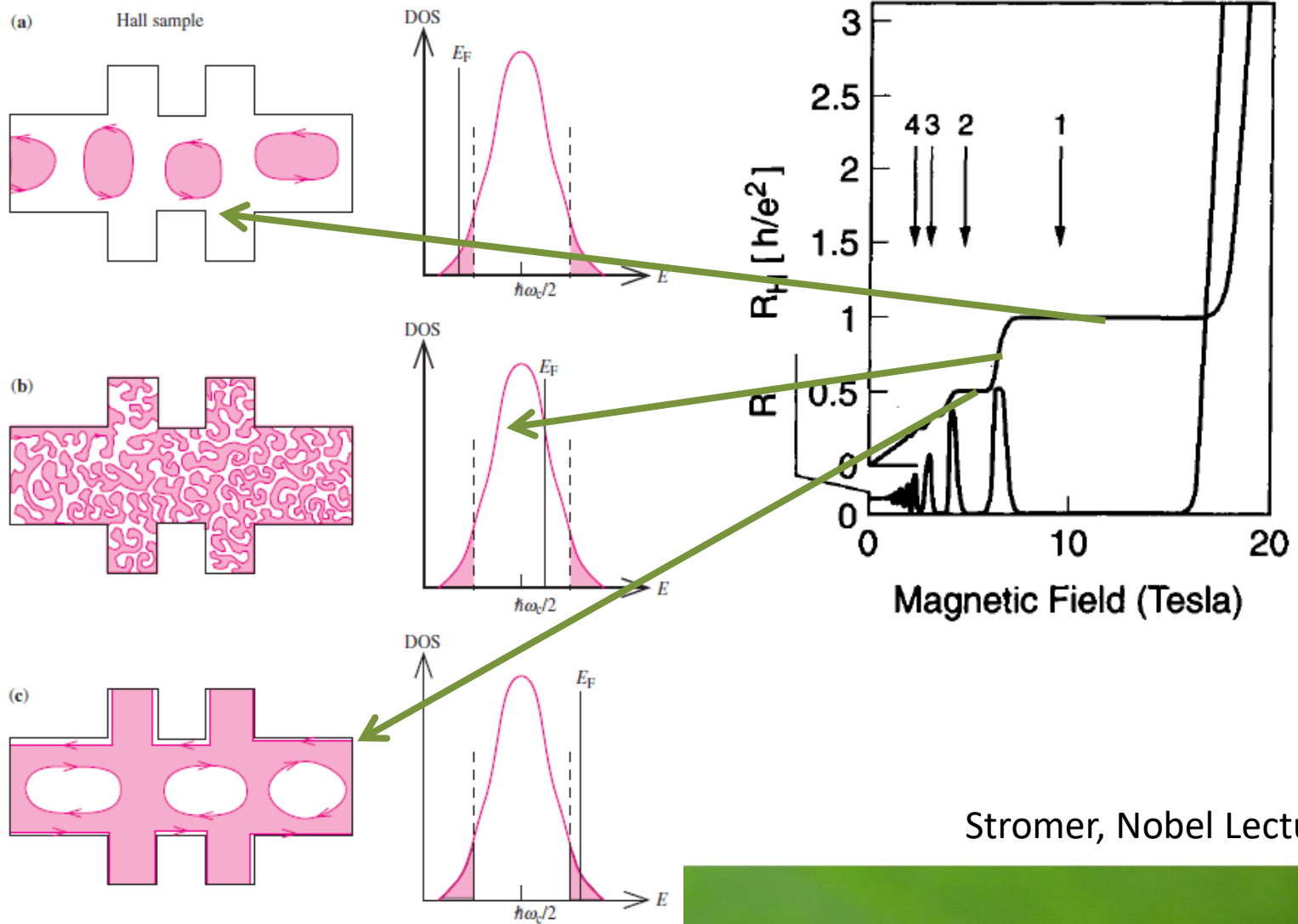
Figure 5.2: Density of states of a 2DEG in magnetic field. By comparing the DOS with and without magnetic field, we can calculate the number of states within each Landau level. From Ferry & Goodnick.

Clive Emary  
Theory of Nanostructures nanoskript.pdf

# Integer Quantum Hall Effect (IQHE)

Integer Quantum Hall effect (IQHE) – for 2D gas: if the Fermi level is located in localized states the Hall resistance (*opór hallowski*) is quantized

$$R_H = \frac{1}{\nu} \frac{h}{e^2}$$



Yu, Cardona

Stromer, Nobel Lecture

# Fractional Quantum Hall Effect (FQHE)

Fractional Quantum Hall Effect (FQHE) – for 2D gas  $\nu \leq 1$ : if the Fermi level is located in localized states the Hall resistance (*opór hallowski*) is quantized

$$R_H = \frac{1}{\nu^*} \frac{h}{e^2}$$

Stromer, Nobel Lecture

# Fractional Quantum Hall Effect (FQHE)

Fractional Quantum Hall Effect (FQHE)  
 Fractional Quantum Hall Effect (FQHE)  
 localized state

$$R_H = \frac{1}{\nu} \frac{h}{e^2}$$

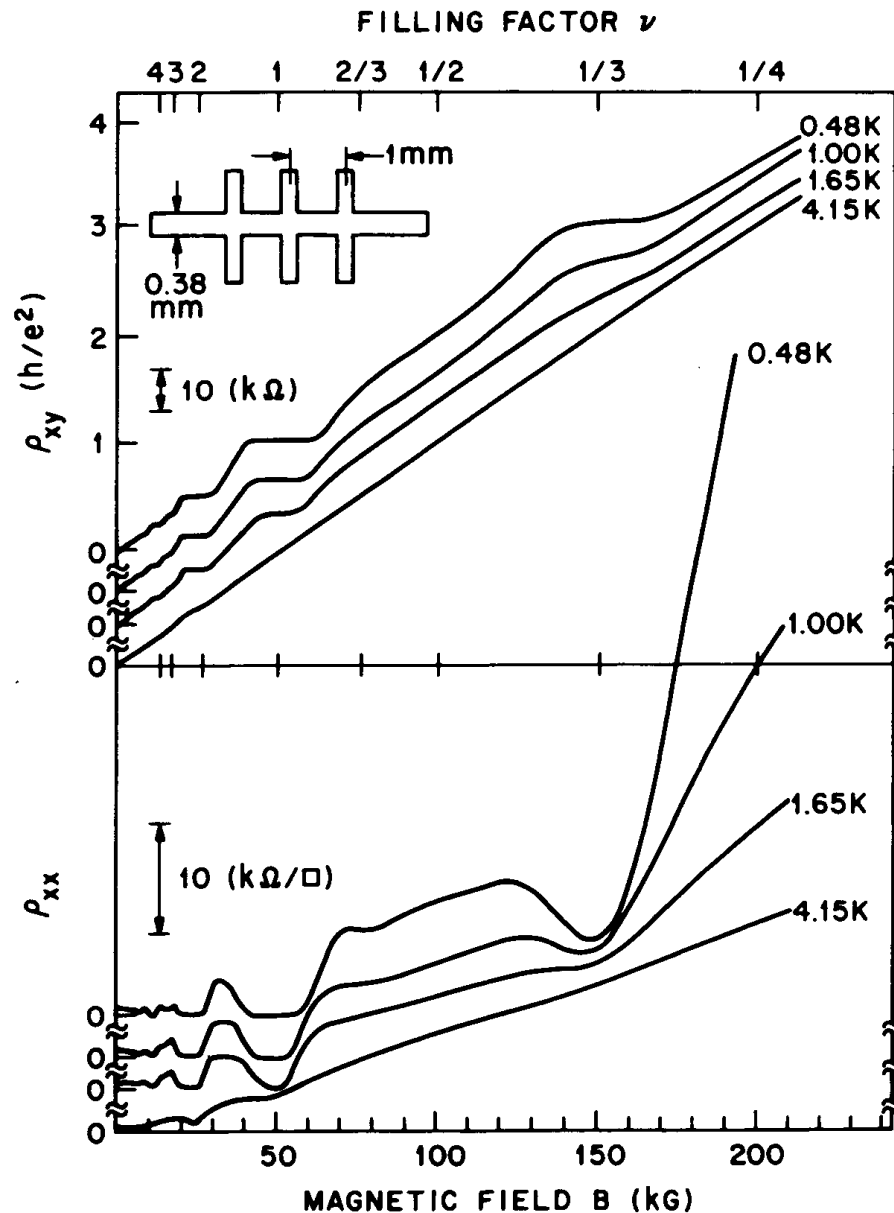


Figure 10. First publication on the FQHE. Hall resistance data (here  $\rho_{xy}$ ) and magneto-resistance data (here  $\rho_{xx}$ ) are from the same specimen as in Fig. 9. The filling factor,  $\nu$ , of the Landau level is indicated on the top. The features at  $\nu=1, 2, 3, \dots$  are due to the IQHE. The features at  $\nu=1/3$  are due to the FQHE. Sample dimensions and sample temperatures are indicated.

# Stromer (FQHE)

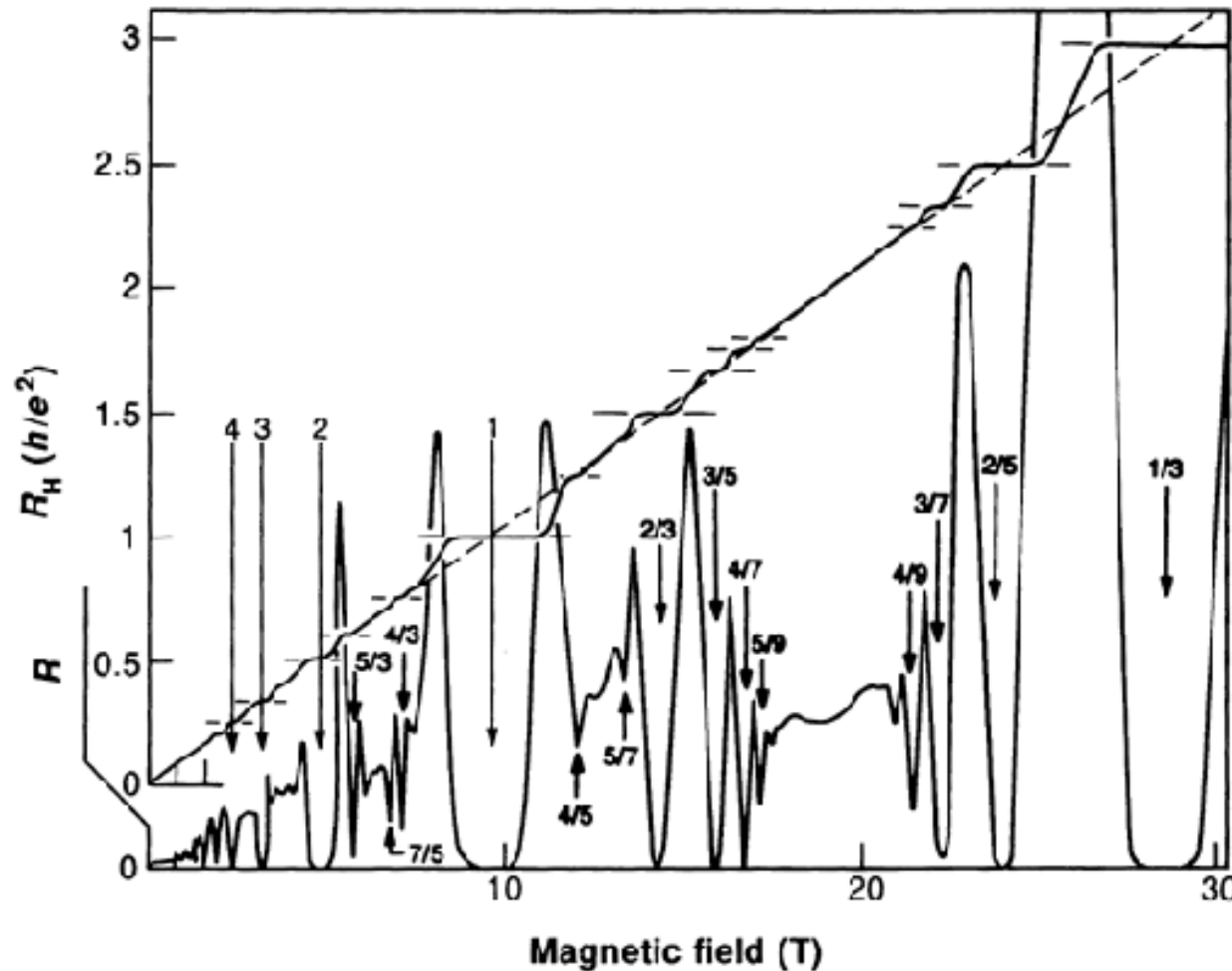
level is located in

Stromer, Nobel Lecture

# Fractional Quantum Hall Effect (FQHE)

Fractional Quantum Hall Effect (FQHE) – for 2D gas  $\nu \leq 1$ : if the Fermi level is located in localized states the Hall resistance (*opór hallowski*) is quantized

$$R_H = \frac{1}{\nu} \frac{h}{e^2}$$



# Fractional Quantum Hall Effect (FQHE)

Fractional Quantum Hall Effect (FQHE) – for 2D gas  $\nu \leq 1$ : if the Fermi level is located in localized states the Hall resistance (*opór hallowski*) is quantized

$$R_H = \frac{1}{\nu^*} \frac{h}{e^2}$$

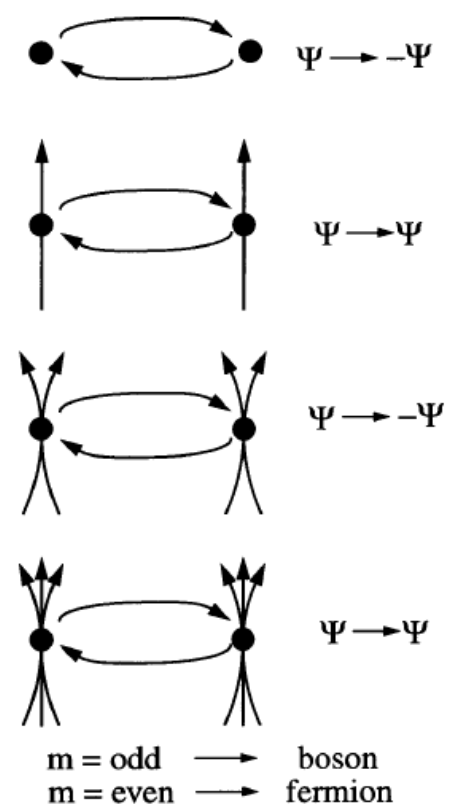
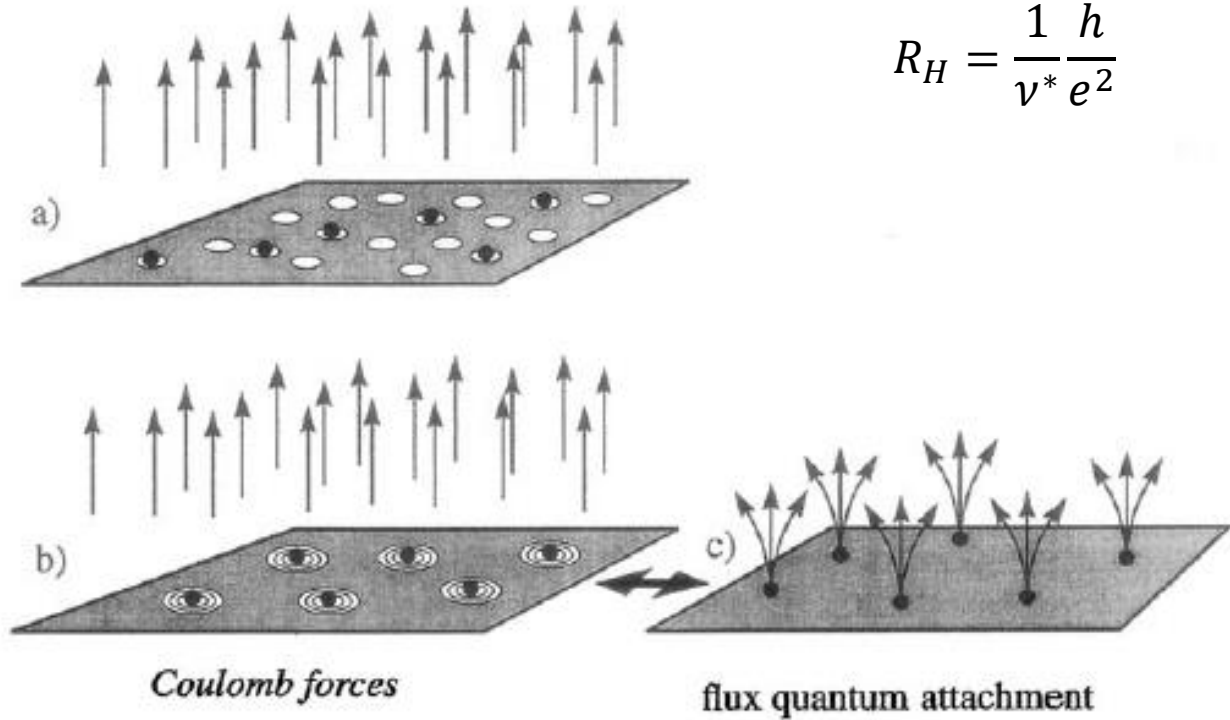


Figure 14. Schematic drawing of electron vortex attraction at fractional Landau level filling,  $\nu=1/3$ . Now there are three times as many vortices as there are electrons. The Pauli principle is satisfied by placing one vortex onto each electron (a). Placing three vortices onto each electron reduces electron-electron (Coulomb) repulsion (b). Vortex attachment can be viewed as the attachment of magnetic flux quanta to the electrons transforming them to composite particles (c).

of electrons and composite particles. Exchange of two particles affects the wavefunction  $\Psi$  which described the quantum-mechanical behavior of the system. For electrons, exchange results in  $\Psi \rightarrow -\Psi$ , identified by  $-1$ , identifying the particles as fermions. With the attachment of an odd number of flux quanta, the wavefunction  $\Psi$  remains *unchanged* under exchange (multiplication by  $+1$ ), identifying the particles as bosons. Attachment of an even number of flux quanta returns the particles to fermions.

Stromer, Nobel Lecture

# Composite fermions

Fractional Quantum Hall Effect (FQHE) – composite fermions, fractionally charged quasiparticles

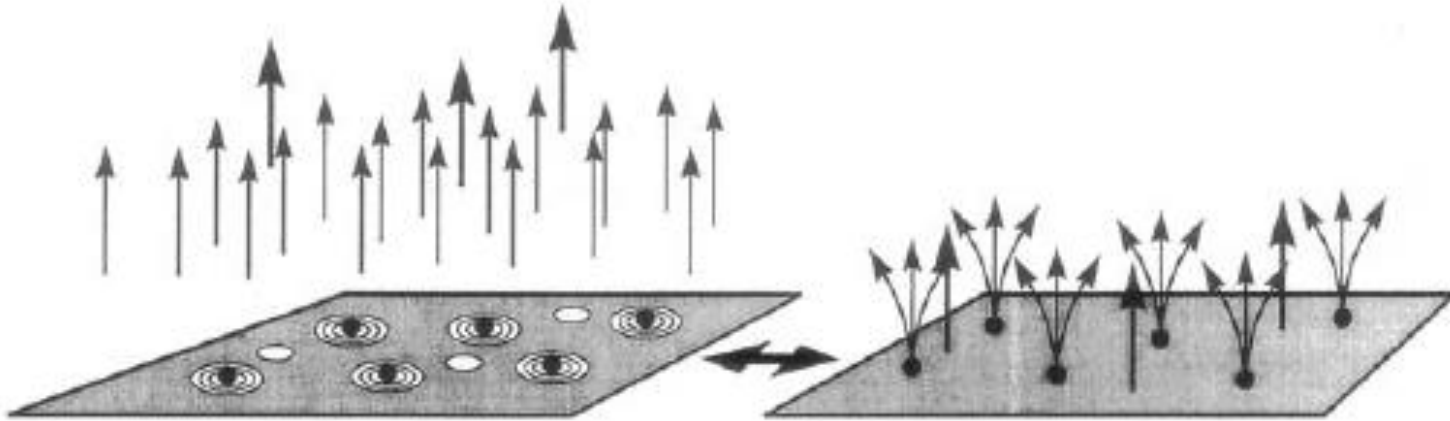
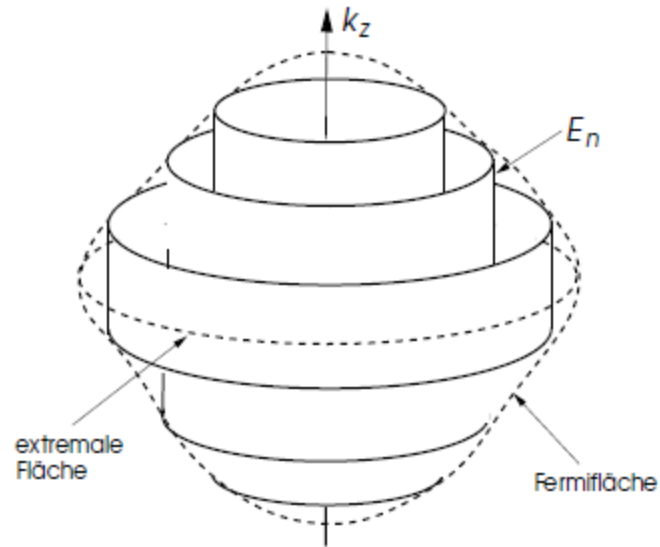


Figure 16. Schematic representation of  $1/3$  charged quasiparticles. At slightly higher B fields than at  $\nu=1/3$  additional vortices are created. They represent dimples in the electron lake. In the dimples exactly  $1/3$  of an electron charge is missing. These are the fractionally charged quasiparticles of the FQHE.

Stromer, Nobel Lecture

# De Haas – van Asphen

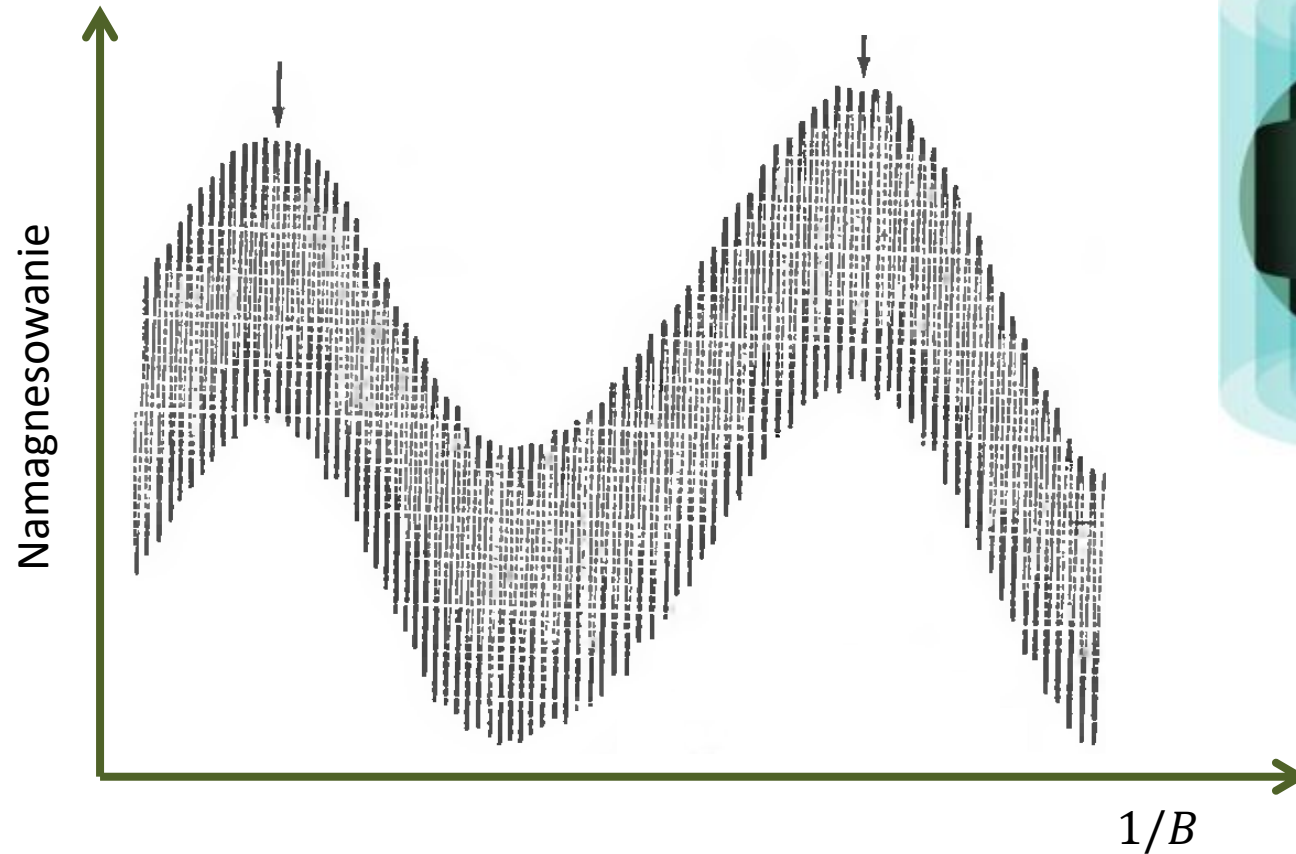


*Fig. 3.12: Tubes of quantized electronic states in a magnetic field along the  $z$ -axis. A maximum of the magnetization occurs every time a tube crosses the extremal Fermi surface area as the magnetic field is increased.*

[www.itp.phys.ethz.ch/education/lectures\\_fs10/Solid/Notes.pdf](http://www.itp.phys.ethz.ch/education/lectures_fs10/Solid/Notes.pdf)

# De Haas – van Asphen

Moment magnetyczny czystego monokryształu metalu oscyluje w zmiennym polu magnetycznym



Ashcroft, Mermin

# De Haas – van Asphen

Moment magnetyczny czystego monokryształu metalu oscyluje w zmiennym polu magnetycznym

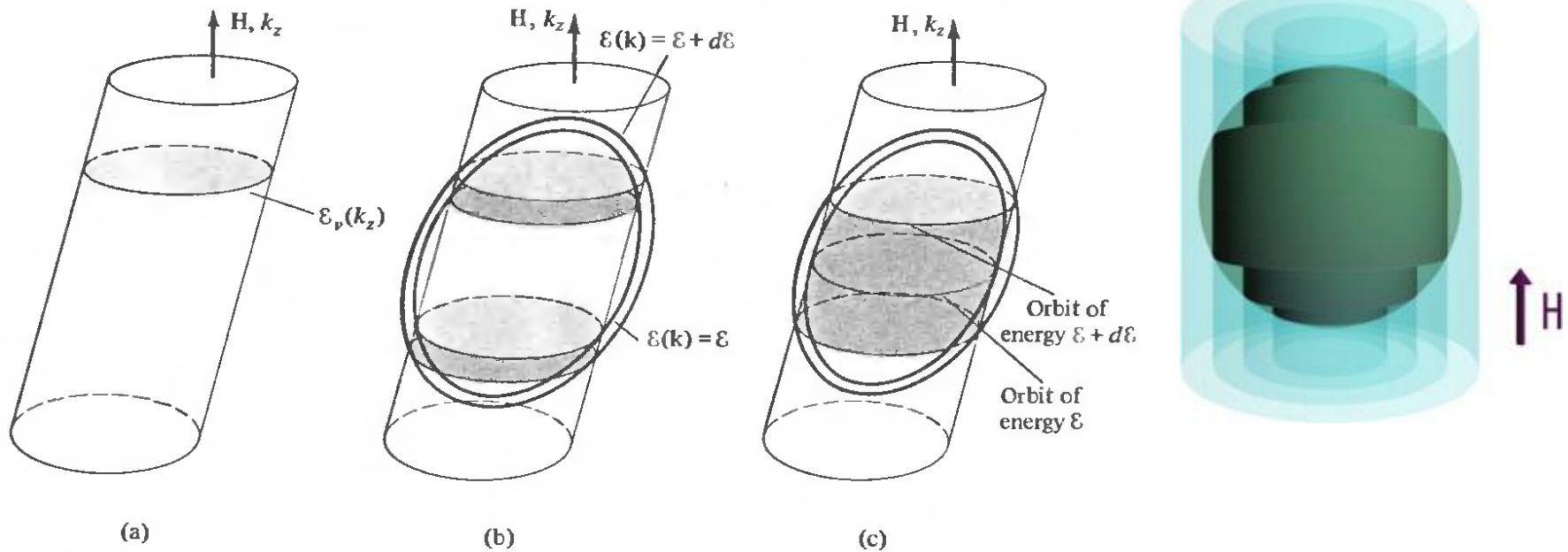


**Figure 14.5**

(a) A Landau tube. Its cross sections by planes perpendicular to  $H$  have the same area— $(v + \lambda) \Delta A$  for the  $v$ th tube—and are bounded by curves of constant energy  $\epsilon_v(k_z)$  at height  $k_z$ . (b) The portion of the tube containing orbits in the energy range from  $\epsilon$  to  $\epsilon + d\epsilon$  when none of the orbits in that range occupy extremal positions on their constant-energy surfaces. (c) Same construction as in (b), except that  $\epsilon$  is now the energy of an extremal orbit. Note the great enhancement in the range of  $k_z$  for which the tube is contained between the constant-energy surfaces at  $\epsilon$  and  $\epsilon + d\epsilon$ .

Ashcroft, Mermin

# De Haas – van Asphen

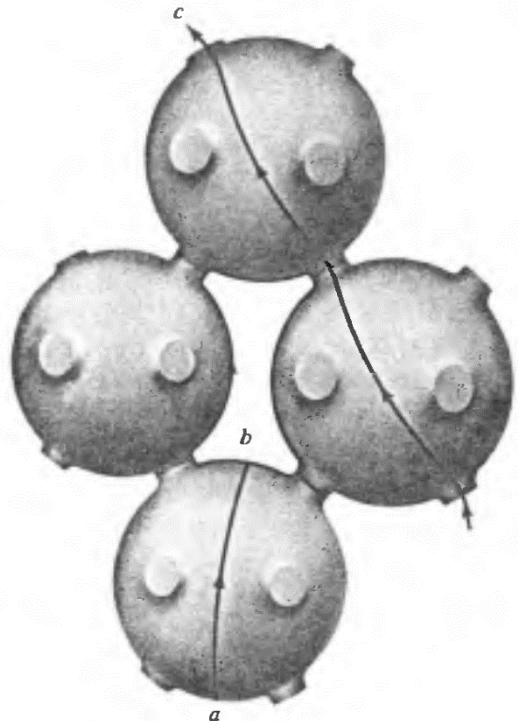


**Figure 15.7**  
 Indicating only a few of the surprisingly many types of orbits an electron can pursue in  $k$ -space when a uniform magnetic field is applied to a noble metal. (Recall that the orbits are given by slicing the Fermi surface with planes perpendicular to the field.) The figure displays (a) a closed particle orbit; (b) a closed hole orbit; (c) an open orbit, which continues in the same general direction indefinitely in the repeated-zone scheme.

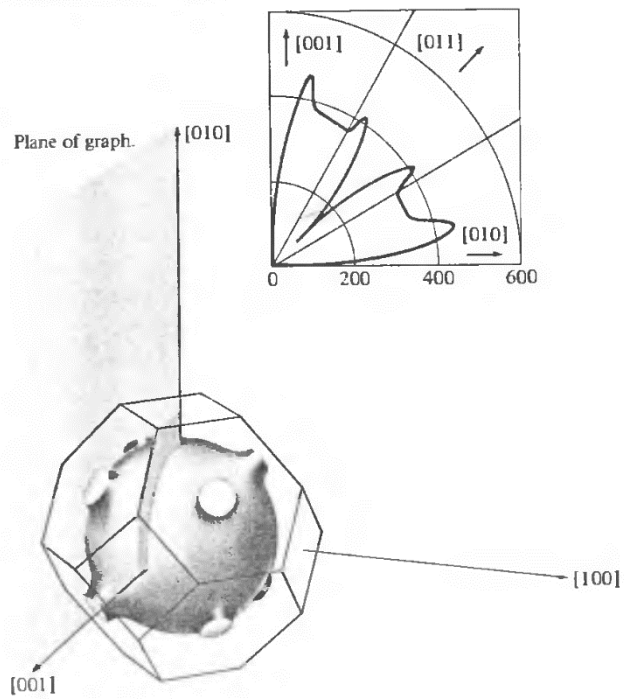


**Figure 15.8**  
 The spectacular direction dependence of the high-field magnetoresistance in copper that is characteristic of a Fermi surface supporting open orbits. The [001] and [010] directions of the copper crystal are as indicated in the figure, and the current flows in the [100] direction perpendicular to the graph. The magnetic field is in the plane of the graph. Its magnitude is fixed at 18 kilogauss, and its direction varied continuously from [001] to [010]. The graph is a polar plot of

$$\frac{\rho(H) - \rho(0)}{\rho(0)}$$

vs. orientation of the field. The sample is very pure and the temperature very low (4.2 K—the temperature of liquid helium) to insure the highest possible value for  $\omega_c\tau$ . (J. R. Klauder and J. E. Kunzler, *The Fermi Surface*, Harrison and Webb eds., Wiley, New York, 1960.)

# De Haas – van Asphen

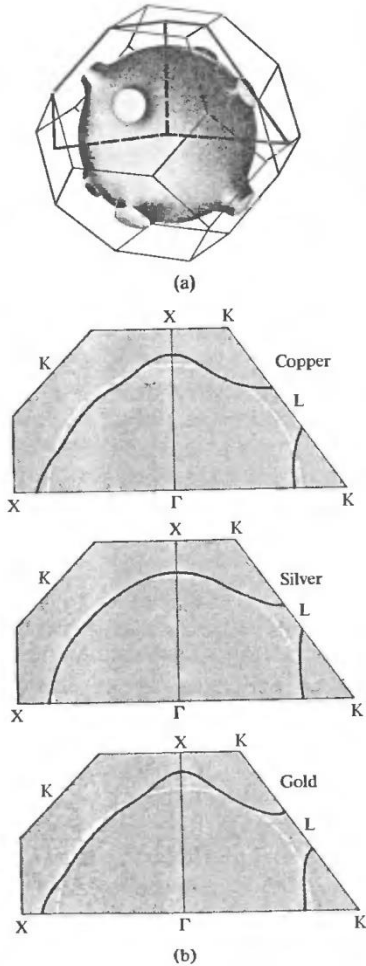


**Figure 15.5**  
 (a) In the three noble metals the free electron sphere bulges out in the  $\langle 111 \rangle$  directions to make contact with the hexagonal zone faces. (b) Detailed cross sections of the surface for the separate metals. (D. Shoenberg and D. J. Roaf, *Phil. Trans. Roy. Soc.* 255, 85 (1962).) The cross sections may be identified by a comparison with (a).

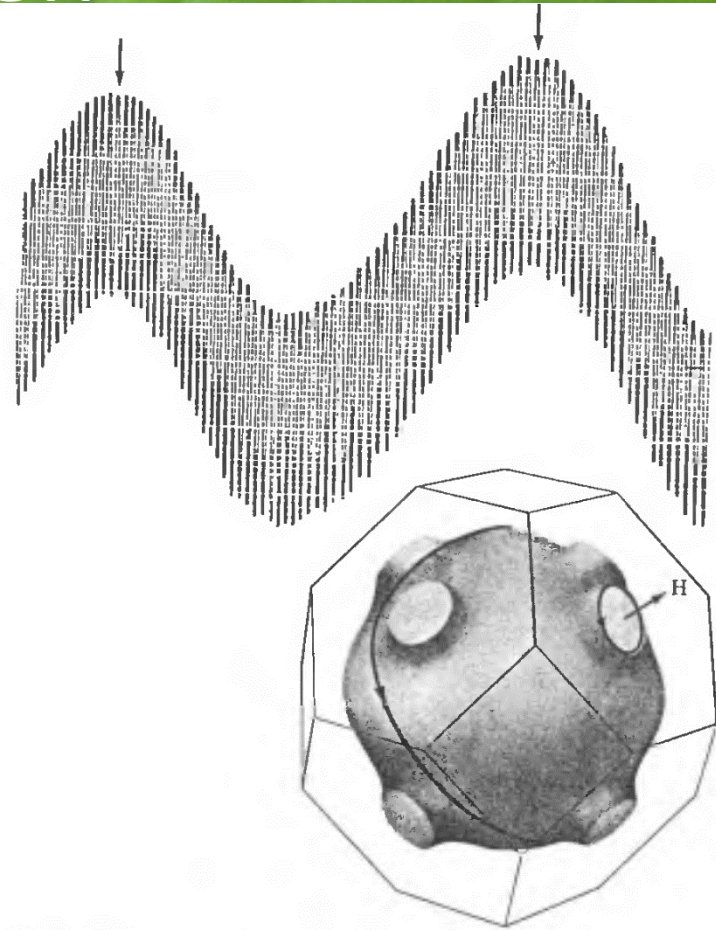


**Figure 15.6**  
 De Haas-van Alphen oscillations in silver. (Courtesy of A. S. Joseph.) The magnetic field is along a  $\langle 111 \rangle$  direction. The two distinct periods are due to the neck and belly orbits indicated in the inset, the high-frequency oscillations coming from the larger belly orbit. By merely counting the number of high-frequency periods in a single low-frequency period (i.e., between the two arrows) one deduces directly that  $A_{111}(\text{belly})/A_{111}(\text{neck}) = 51$ . (Note that it is not necessary to know either the vertical or horizontal scales of the graph to determine this fundamental piece of geometrical information!)



fot. AcidCow.com